

Taper-less III-V/Si Hybrid MOS Optical Phase Shifter using Ultrathin InP Membrane

Shuhei Ohno¹, Qiang Li¹, Naoki Sekine¹, Junichi Fujikata², Masataka Noguchi², Shigeki Takahashi², Kasidit Toprasertpong¹, Shinichi Takagi¹, and Mitsuru Takenaka¹

¹Department of Electrical Engineering and Information Systems, The University of Tokyo, 7-3-1 Hongo, Bunkyo-ku, Tokyo, 113-8656, Japan

²Photonics Electronics Technology Research Association (PETRA), Tsukuba, Ibaraki 305-8569, Japan
ohno@mosfet.t.u-tokyo.ac.jp

Abstract: We present proof-of-concept taper-less III-V/Si hybrid MOS optical phase shifter. An ultrathin InP membrane enables low insertion loss despite no taper, with keeping high modulation efficiency owing to strong electron confinement at the MOS interface. © 2020 The Author(s)

OCIS codes: (130.3120) Integrated optics devices; (230.4110) Modulators.

1. Introduction

Programmable nanophotonic processors (PNPs) based on silicon photonic integrated circuits (PICs) has attracted a lot of attention for signal processing, switching, sensing as well as computing including deep learning and quantum computing [1-3]. Since a low-power, low-loss, and high-speed optical phase shifter is essential for large-scale PNPs, we have proposed to use a III-V/Si hybrid metal-oxide-semiconductor (MOS) optical phase shifter for PNPs [4]. As shown in Fig. 1(a), a III-V/Si hybrid MOS optical phase shifter consists of an n-type III-V membrane bonded on a p-type Si waveguide with gate oxide. A gate voltage applied between the III-V membrane and Si waveguide induces electron accumulation at the III-V MOS interface, resulting in efficient and low-loss phase modulation [5], suitable for low-power optical switching in PNPs [6]. However, in previous studies, 160-nm to 220-nm thick III-V membrane required 50- μm -long tapers at the both input and output of the phase shifter to obtain smooth optical mode transition between the Si waveguide and hybrid waveguide as shown in Fig. 1(a). For large-scale integration, it is preferable to minimize the total length of the tapers. In this paper, we propose to use an ultrathin III-V membrane bonded on a SiO₂-embedded Si waveguide, enabling a taper-less III-V/Si hybrid MOS optical phase shifter as shown in Fig. 1(b). Since the thickness of the electron accumulation layer at the III-V MOS interface is very thin, we expect that sound optical phase modulation is still possible. We have numerically analyzed the impact of an ultrathin III-V membrane on the insertion loss and modulation efficiency. We have also demonstrated a proof-of-concept taper-less III-V/Si hybrid MOS optical phase shifter with a 30-nm-thick InP membrane.

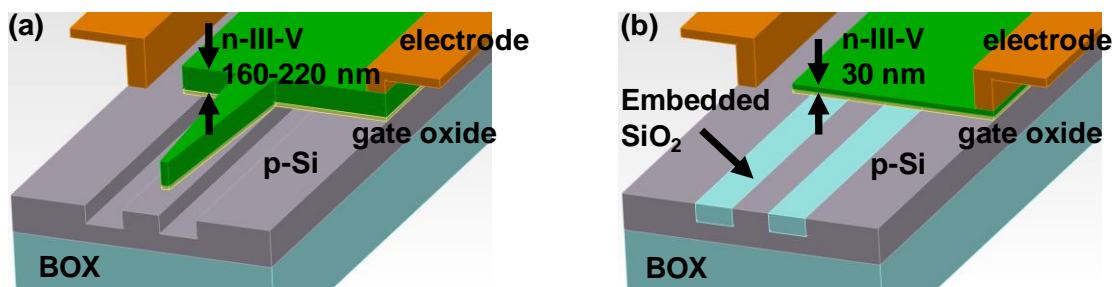


Fig. 1. (a) III-V/Si hybrid MOS optical phase shifter studied previously [4-6] and (b) taper-less III-V/Si hybrid MOS optical phase shifter with an ultrathin III-V membrane.

2. Numerical analysis

We numerically analyzed taper-less III-V/Si hybrid MOS optical phase shifter at a 1550 nm wavelength with varied thicknesses of an InP membrane as shown in Fig. 2(a). We assumed a 400-nm-wide and 200-nm-high Si rib waveguide. First, we performed finite-difference time-domain (FDTD) simulation to evaluate the insertion loss from a Si waveguide and a hybrid phase shifter. Figure 2(b) shows a relationship between the thickness of the InP membrane and the insertion loss. When the InP thickness decreased from 220 nm to 20 nm, the insertion loss decreased from 1.28 dB to 0.03 dB. Figure 2(c) shows simulation results of the transmission of the optical field from the Si waveguide to the hybrid waveguide when the thickness of the InP membrane were 220 nm and 40 nm, respectively. By using an ultrathin InP membrane, we can suppress multimode transmission in the hybrid waveguide, resulting in the low insertion loss. Next, we analyzed the modulation efficiency based on overlap between the optical mode and accumulated electrons and holes at the MOS interfaces. An equivalent oxide thickness (EOT) of the MOS

capacitor was assumed to be 5 nm. Figure 3(a) shows the optical power profile of the fundamental transverse electric (TE) mode and the distributions of electron and hole when the thickness of the InP membrane is 40 nm. As we expect, the accumulated electrons are well confined even in the 40-nm-thick InP membrane. Figure 3(b) shows the modulation efficiency $V_{\pi}L$ as a function of the InP thickness. Even when the InP thickness is reduced to 40 nm, $V_{\pi}L$ is expected to be lower than 0.2 Vcm, which is better than state-of-the-art Si MOS optical modulator [7].

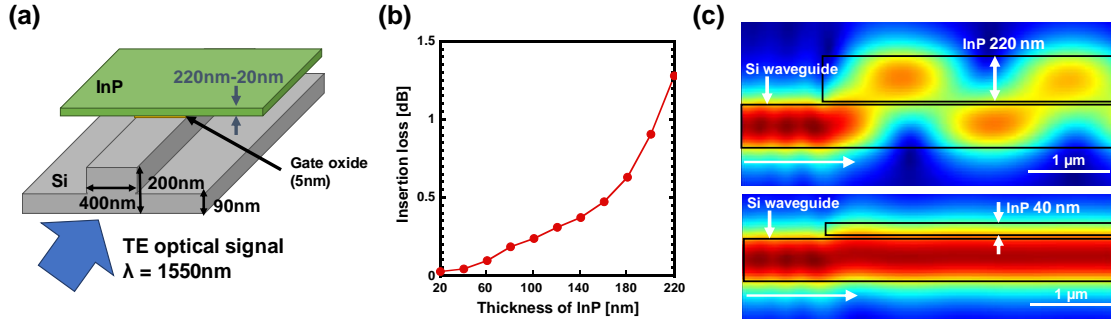


Fig. 2. FDTD simulation of taper-loss III-V/Si hybrid MOS optical phase shifter. (a) Device structure. (b) Insertion loss. (c) Transmission from Si waveguide to hybrid waveguide.

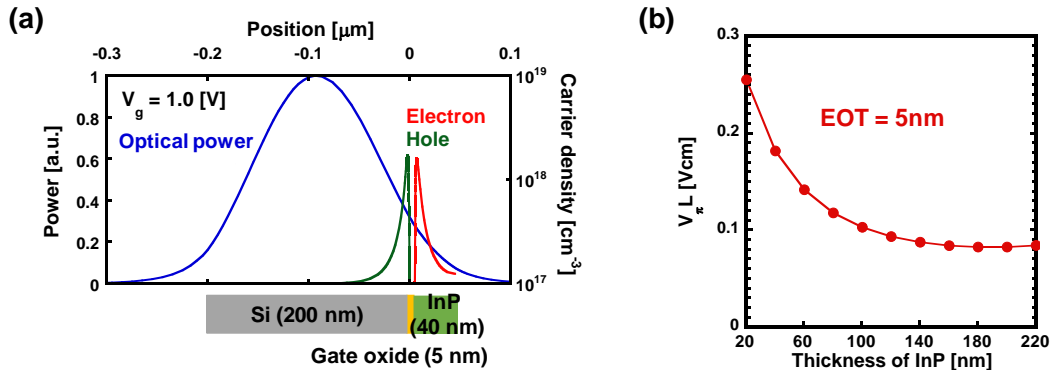


Fig. 3. (a) Optical power profile of the fundamental TE mode and carrier distributions in the hybrid phase shifter with a 40-nm-thick InP membrane. (b) Relationship between modulation efficiency and InP thickness.

3. Device fabrication and evaluation

We fabricated asymmetric Mach-Zehnder interferometer (AMZI) with taper-less III-V/Si hybrid optical phase shifter using a 30-nm-InP membrane. Figures 4(a) to 4(c) shows the fabrication procedure. After forming Si rib waveguides, SiO₂ was deposited by chemical vapor deposition. Then, the surface was planarized by chemical mechanical polishing (CMP) to obtain the SiO₂-embedded Si waveguide. Ion implantation was carried out to form p-doped Si regions for the phase shifters. Ion implantation of Si was also performed for a 30-nm-InP layer grown on an InP substrate followed by activation annealing at 650 °C for 3 min. The implanted InP epitaxial wafer were bonded with Al₂O₃ gate oxide. Then, the InP substrate and a 1000-nm-thick InGaAs etch-stop layer were removed followed by III-V mesa etching. After the deposition of SiO₂ as a cladding layer, electrodes were formed. Since the gate oxide consisted of 15 nm SiO₂ and 6 nm Al₂O₃, an estimated EOT of the hybrid MOS capacitor was 18 nm. It can be seen in Fig. 5(a) that the InP membrane was bonded on the SiO₂-embedded Si waveguide with no taper. The length of phase shifter was 240 μm. The difference in the length of the two MZI arms was 20 μm. Figure 5(b) shows the transmission spectra with varied gate voltages.

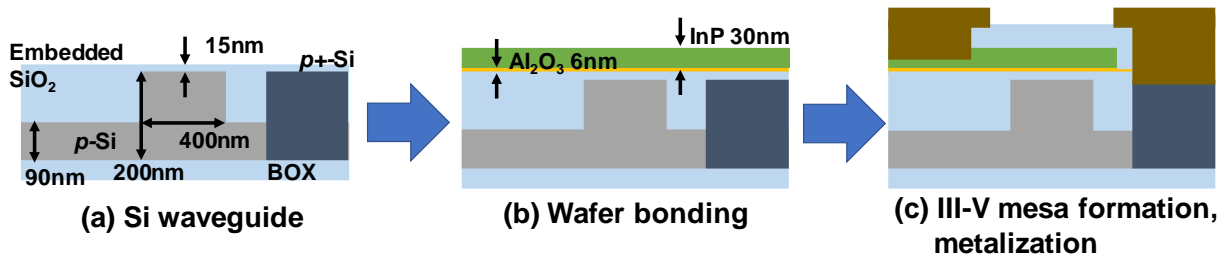


Fig. 4. Fabrication process of taper-less III-V/Si hybrid MOS optical phase shifter.

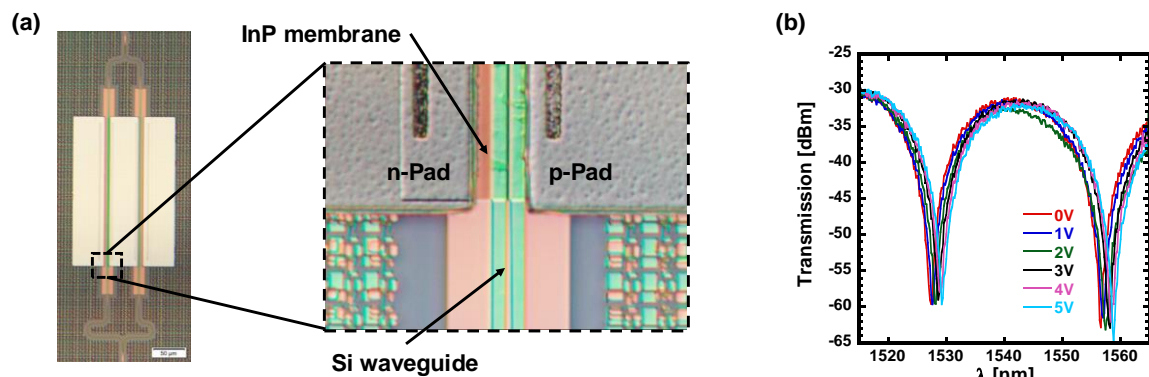


Fig. 5. (a) Microscope image and (b) output spectra of fabricated taper-less III-V/Si hybrid MOS optical phase shifter.

Fig. 6(a) shows the amount of the phase shift extracted from Fig. 5(b). The modulation efficiency was 0.77 Vcm, which agreed with the simulation result in case of 18 nm EOT. To evaluate the reflection of the hybrid waveguide, inverse Fourier transform (IFT) was performed on its transmission spectrum. As shown in Fig. 6(b), we observed no specific peak except for the peak at 20 μm corresponding to the difference in the arm length of the AMZI, suggesting negligible reflection as expected. Figure 6(c) shows the relationship between EOT and $V_{\pi}L$ when the thickness of the III-V membrane is 30 nm. By reducing the EOT down to 5 nm and introducing InGaAsP ($\lambda_g = 1.37 \mu\text{m}$) instead of InP, we can achieve $V_{\pi}L$ around 0.1 Vcm, promising for PNPs.

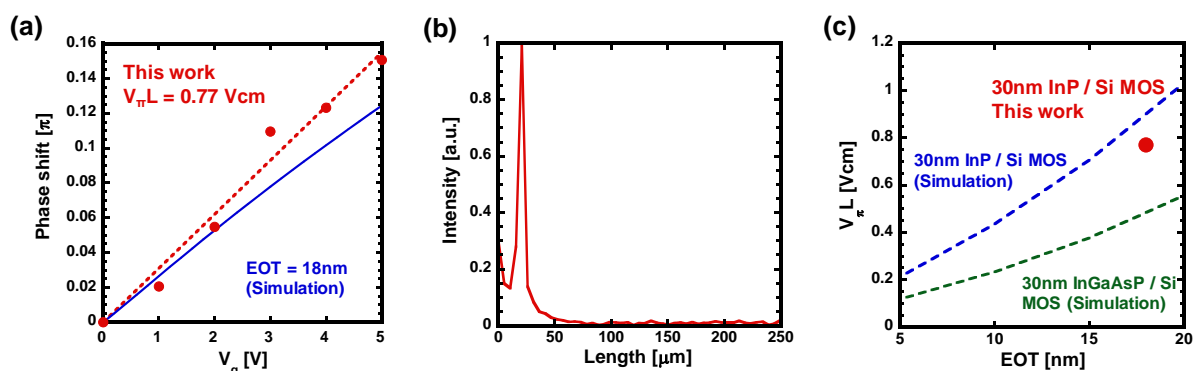


Fig. 6. (a) Phase shift obtained from Fig. 5(c). (b) IFT analysis of the transmission spectrum. (c) Relationship between EOT and modulation efficiency when the thickness of III-V membrane is 30 nm.

4. Conclusions

We proposed taper-less III-V/Si hybrid MOS optical phase shifter using an ultrathin InP membrane. We numerically revealed that an ultrathin InP membrane enable the insertion loss less than 0.1 dB with no taper and the modulation efficiency can be kept rather high even thinning InP membrane owing to the strong confinement of accumulated electrons at the MOS interface. We have also successfully shown proof-of-concept taper-less III-V/Si hybrid MOS optical phase shifter by bonding a 30-nm-thick InP membrane on the SiO_2 -embedded Si waveguide, applicable to large-scale PNPs.

Acknowledgements

This work was partly commissioned by the New Energy and Industrial Technology Development Organization (NEDO).

References

- [1] Y. Shen et al., "Deep learning with coherent nanophotonic circuits," *Nat. Photon.*, **11**, 441-446 (2017).
- [2] L. Zhuang et al., "Programmable photonic signal processor chip for radiofrequency applications," *Optica*, **2**, 854-859 (2015).
- [3] N. C. Harris et al., "Quantum transport simulations in a programmable nanophotonic processor," *Nat. Photon.*, **11**, 447-452 (2017).
- [4] M. Takenaka et al., "III-V/Si Hybrid MOS Optical Phase Shifter for Si Photonic Integrated Circuits," *J. Lightwave Technol.* **37**, 1474-1483 (2019).
- [5] J.-H. Han et al., "Efficient low-loss InGaAsP/Si hybrid MOS optical modulator," *Nat. Photon.*, **11**, 486-490 (2017).
- [6] Q. Li et al., "Ultra-power-efficient 2 x 2 Si Mach-Zehnder interferometer optical switch based on III-V/Si hybrid MOS phase shifter," *Opt. Express* **26**, 35003-35012 (2018).
- [7] J. Fujikata et al., "High-speed and high-efficiency Si optical modulator with MOS junction, using solid-phase crystallization of polycrystalline silicon," *Jpn. J. Appl. Phys.* **55**, 042202 (2016).